FA increased over time in the degraded patch but not in the control patch (*15*).

More mobile species showed a significantly higher level of persistence than less mobile species after correction for the effects of change in asymmetry, i.e., they occupied a higher proportion of patches than expected from their estimated stress sensitivity (Fig. 1A). Highly comparable results (*19*) were obtained when we used the estimates of recapture rate and constant dispersal probability listed in Table 1. Change in asymmetry, in turn, significantly explained residual variance in patch occupancy (Fig. 1B), i.e., less sensitive species occupied a higher proportion of patches than predicted from their estimated level of mobility (*20*). Together, dispersal rate and change in asymmetry explained 88% of the observed variation in patch occupancy between species, with each factor contributing equally to the relationship (45% of the variation was explained by probability of dispersal; 43% of the variation was explained by change in asymmetry).

On the basis of these results, we conclude that individual-level parameters, such as mobility and developmental homeostasis, can be scaled up to predict species-specific patterns at landscape level [the "behavioral ecology of ecological landscapes" concept (*21*)]. In a comparable approach, models have been developed that scale mass-related energy requirements with population density (*22*). The use of simple, accurate, and cost-effective biomarkers, such as individual asymmetry, further permits us to measure the impact of environmental stress and to take appropriate conservation action before species become irreversibly affected [the "early warning" concept (*23*, *24*)]. Application of such an individual-level approach, in part of one of the world's most threatened biodiversity hotspots, suggests that conservation tactics may fail unless they include action both within sites, to minimize habitat deterioration, and across landscapes, to maximize dispersal.

References and Notes

1. G. R. Robinson, F. R. Thompson III, T. M. Donovan, D. R. Whitehead, J. Faaborg, *Science* **257**, 524 (1992).
2. M. L. Hale *et al.*, *Science* **293**, 2246 (2001).
3. R. S. Etienne, J. A. P. Heesterbeek, *Am. Nat.* **158**, 389 (2001).
4. N. Myers, R. A. Mittermeier, C. G. Mittermeier, G. A. B. da Fonseca, J. Kent, *Nature* **403**, 853 (2000).
5. A selection of maps of the study area, illustrating its global position, its elevational structure, and spatial relationships of the forest fragments, can be found at http://bio-www.uia.ac.be/bio/deco/topics.html#study areas.
6. P. Dias, *Trends Ecol. Evol.* **11**, 326 (1996).
7. Occupancy was calculated as the proportion of small forest fragments (n_{tot} = 9) with confirmed breeding activity during one or more breeding seasons between 1996 and 2001.
8. G. White, K. P. Burnham, *Bird Study* **S46**, 120 (1999).
9. Individual recapture histories were generated using time intervals of 1 month. Such a short time interval was needed because over longer intervals (3, 6, or 12 months), a number of individuals were recaptured in multiple forest fragments within a single interval. A total of 889 individuals were captured-recaptured in two or more months, and among these, 47 individuals were captured-recaptured in two or more fragments.
10. We used Akaike's Information Criteria (AIC) to determine the most parsimonious model among a candidate set and computed species-specific dispersal probabilities for further analysis from this model. Recapture data were too sparse to include fully time-dependent models of survival and recapture probabilities in the candidate set of models, and sample size did not allow us to calculate complex multistrata models for *Apalis thoracica*. For this species, no single individual was captured in more than one fragment, hence Ψ was estimated as 0. There is no formal goodness-of-fit test for multistrata models, yet our results were robust for a range of 1 to 1.5 in the overdispersion parameter $\hat{c}$.
11. More complex dispersal models could not be fitted to all species in MARK because models were overparameterized. For the more mobile species with adequate numbers of recaptures after dispersal between fragments, a model assuming direction-dependent dispersal rates between fragment pairs fitted the recapture data significantly better than the direction-independent model described in Table 1 for two species, but equally as well as the direction-independent model for two other species (nested models were compared using likelihood ratio tests).
12. L. Van Valen, *Evolution* **16**, 125 (1962).
13. L. Lens, S. Van Dongen, S. Kark, E. Matthysen, *Biol. Rev.* **77**, 27 (2002).
14. S. Van Dongen, G. Molenberghs, E. Matthysen, *J. Evol. Biol.* **12**, 94 (1999).
15. L. Lens, S. Van Dongen, C. M. Wilder, T. M. Brooks, E. Matthysen, *Proc. R. Soc. London Ser. B* **266**, 1241 (1999).
16. The validity of this relationship depends on the assumption that tarsi develop in the patch where they are measured. Violation of this assumption, however, can only bias results against the hypothesis tested in this paper.
17. No museum samples were available for *A. thoracica* (rare species) and *Nectarinia olivacea* (abundant species yet not collected in the Taita Hills).
18. Estimates of relative change in FA were obtained from the random species × time interaction (χ^2_1 = 4.1, $P < 0.05$) in a three-way mixed analysis of variance with unsigned FA as the dependent variable; fragment as a fixed factor; and species, time, and all relevant two- and three-way interaction terms as random factors [model specifications in (*15*)].
19. L. Lens, S. Van Dongen, K. Norris, M. Githiru, E. Matthysen, data not shown.
20. Logistic regression analysis was performed in WINBUGS version 1.3 to allow for missing values and use of all available data [W. R. Gilks, A. Thomas, D. J. Spiegelhalter, *The Statistician* **43**, 169 (1994)]. The occupancy-dispersal association was based on eight species and the occupancy-asymmetry association on six species. An extra dispersion variance parameter [parameter estimate 0.22 ± 0.71, 95% confidence interval (CI) 0.001 to 1.63] was added to correct for overdispersion (*25*).
21. S. L. Lima, P. A. Zollner, *Trends Ecol. Evol.* **11**, 131 (1996).
22. C. Carbone, J. L. Gittleman, *Science* **295**, 2273 (2002).
23. G. M. Clarke, *Conserv. Biol.* **9**, 18 (1995).
24. L. Lens, S. Van Dongen, E. Matthysen, *Conserv. Biol.* **16**, 479 (2002).
25. P. Congdon, *Bayesian Statistical Modelling* (Wiley, Chichester, UK, 2001).

26. We thank B. Amakobe, J. Barnes, R. Barnes, T. Brooks, A. Cooke, D. Gitau, T. Imboma, C. Jackson, J. Kageche, S. Karimi, J. Lindsell, G. Mwachala, D. Samba, E. Waiyaki, C. Wilder, and the staff of the Taita-Taveta District Forest Department, the Ornithology Department of the National Museums of Kenya, and the East African Herbarium for help with fieldwork. B. Bytebier and M. De Meyer of the Taita Hills Biodiversity Project provided logistic support. L. Bennun, P. Sweet, J. Bates, D. Willard, R. Paynter, and F. Sibley allowed access to the historical specimens. A. Notenbaert and S. Vanlishout provided help with the compilation of maps of the study area. Supported by the Fund for Scientific Research Flanders (L.L., S.V.D.) and Flemish Interuniversity Council project 02/6/7-338-607 (E.M.).

2 July 2002; accepted 27 August 2002

The Control of Spikelet Meristem Identity by the *branched silkless1* Gene in Maize

George Chuck,[1,4]* Michael Muszynski,[2] Elizabeth Kellogg,[3] Sarah Hake,[1] Robert J. Schmidt[4]

Most of the world's food supply is derived from cereal grains that are borne in a unique structure called the spikelet, the fundamental unit of inflorescence architecture in all grasses. *branched silkless1* (*bd1*) is a maize mutation that alters the identity of the spikelet meristem, causing indeterminate branches to form in place of spikelets. We show that *bd1* encodes a putative ERF transcription factor that is conserved in different grasses and is expressed in a distinct domain of the spikelet meristem. Its expression pattern suggests that signaling pathways regulate meristem identity from lateral domains of the spikelet meristem.

Development in plants depends primarily on the activity of meristems, indeterminate cell populations whose derivatives form lateral organs. Meristems can be considered determinate or indeterminate, depending on whether they are consumed in the production of lateral primordia. Grass species have evolved unique meristem fates that are central to orchestrating the diverse inflorescence architecture found in this extensive family (*1*, *2*).

Both the male and female inflorescence meristems of maize (tassel and ear, respectively) produce spikelet meristems, determinate branches that produce two glumes and two florets before undergoing sexual specialization (*2*). *bd1* mutants show a loss of determinacy in the maize ear,

with branches found in place of female spikelets (*3, 4*) (Fig. 1; compare A and B). In the *bd1-N2355* (*bd1-N*) tassel, spikelets appear indeterminate and produce a series of lateral spikelets (Fig. 1; compare C and D). All five *bd1* alleles examined displayed similar tassel phenotypes but differed in severity in the ear. The weak *bd-mum::20250* allele initiated fewer branches in the ear, compared with the other alleles, and was able to form a few fertile florets, whereas the most severe alleles converted almost all the initial spikelets to indeterminate branches.

To establish identity of the altered meristems in *bd1* mutants, we carried out scanning electron microscopy (SEM). In wild type, the first 5 to 15 lateral primordia initiated by the tassel inflorescence meristem (IM) are called branch meristems (BMs) (*2*) (Fig. 1, E and F). The tassel IM then produces spikelet pair meristems (SPMs), which form two spikelet meristems (SMs). BMs also produce SPMs, but in a distinct two-ranked (distichous) phyllotaxy. SMs initiate an outer and inner glume, as well as two florets (fig. S1). The ear undergoes these same branching processes, except that BMs are not initiated. Thus, the identity of the meristems can be defined based on their activities: BMs form SPMs in a distichous phyllotaxy; each SPM forms two SMs; and SMs initiate a pair of glumes before forming two floral meristems.

Both the IM and SPM appear normal in *bd1-N* tassels and ears. Defects are first seen in the mutant after SMs are made. In *bd1-N* ears, the presumptive SMs often fail to initiate an outer glume and, instead, indeterminately produce SPMs in a distichous pattern (Fig. 1, G and H). These SPMs form two SMs, each of which initiates outer glumes (Fig. 1I) and then ceases development. Given that the presumptive SMs initiate SPMs in a distichous phyllotaxy, we propose that their identity is converted to a BM identity (Fig. 1; compare F with J). From this phenotype, we hypothesize that one role of BD1 is to repress BM identity within the SMs of the ear.

In the *bd1-N* mutant tassel primordia, SMs initiate an outer glume (Fig. 1K), initiate a meristem in the axil of that glume, and then continue this pattern indeterminately, as revealed by SEM (Fig. 1, L and M). Later, each of these axillary meristems initiates floral organs (Fig. 1N). The identity of the mutant meristem can be considered BM-like because it initiates a series of spikelets indeterminately, although the spikelets are not in pairs. We conclude that BD1 functions to repress indeterminate branching in both inflorescences, but its absence has different consequences, possibly owing to other genetic factors.

The *BD1* gene was cloned by transposon tagging with *Mutator* (*Mu*) (*5*). The sequence flanking a cosegregating *Mu1* element revealed an open reading frame that encodes a putative protein of 315 amino acids with similarity to the ethylene-responsive element–binding factor (ERF) class of transcription factors (Fig. 2A). Analysis of mutant alleles revealed a frameshift mutation upstream of the ERF domain that resulted in a premature stop codon in *bd1-2*, a transition mutation within the ERF domain that introduces a premature stop codon in *bd1-N*, and a deletion of the 3′ end of the gene that is predicted to remove the last 10 amino acids in *bd1-3* (fig. S1).

A related gene, *bd1b,* was cloned from a bacterial artificial chromosome (BAC) library and mapped to chromosome 2L, which is likely to be a segmental duplication of chromosome 7L where *bd1* maps (*6*); this suggests that it is a duplicate locus. Similar *bd1* genes were cloned from rice and sorghum BAC libraries, and from *Setaria italica* (foxtail millet), *Panicum miliaceum* (common millet), *Avena sativa* (oats), and *Eleusine coracana* (finger millet) by polymerase chain reaction (PCR) with degenerate primers. All members of the *bd1* gene family in grasses have complete amino acid identity within the ERF domain and 45 to 75% identity overall (Fig. 2A). A maximum likelihood tree (Fig. 2D) indicates that the genes have evolved largely in accordance with the species tree (*7*), which is consistent with a hypothesis of conserved function. In contrast, *bd1b* shows an accelerated rate of evolution, retaining an open reading frame and the conserved ERF domain, but elsewhere diverging in sequence from *bd1.* This rapid accumulation of mutations suggests a change or loss of function in *bd1b.*

The ERF domain is a plant-specific DNA binding motif (*8*). ERF containing transcription factors function in ethylene-mediated pathogen response as well as cold and abiotic stress responses (*9*). In *Arabidopsis*, two dominant developmental mutants result from ectopic expression of ERF genes. One is *leafy petiole,* which causes the leaf blade to extend down the petiole (*10*), and the other is *tiny*, which causes severe dwarfism (*11*). Overexpression of another related *Arabidopsis* ERF gene, *ESR1* (*12*), confers cytokinin-independent regeneration of shoots from callus tissue, which indicates that some of these

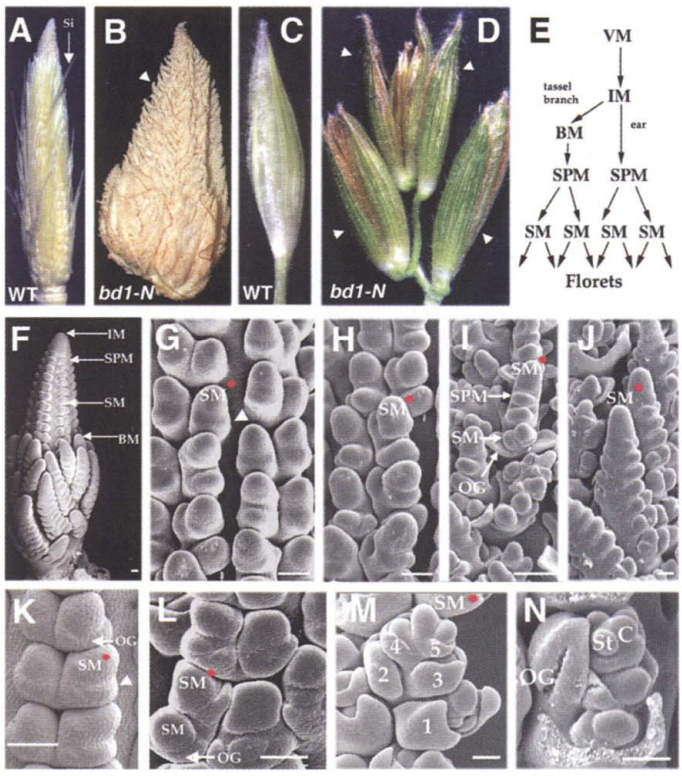

Fig. 1. Wild-type and *bd1-N* mutant tassel and ear spikelets. (**A**) Wild-type OH43 ear with initiating pistil primordia. The ear is normally unbranched. (**B**) *bd1* ear showing the development of multiple branches (arrowhead). (**C**) Single wild-type tassel spikelet. (**D**) Single *bd1* tassel spikelet structure. Arrowheads mark spikelets that branch laterally from other spikelets. (**E**) Schematic of branching in wild-type maize tassels and ears. (**F**) SEM of wild-type tassel primordium. (**G** to **J**) SEM of *bd1* mutant ear. (G) Presumptive SM (marked with red star) is initiating primordia (arrowhead). (H) The SM is initiating primordia distichously. (I) The initiated primordia have SPM activity. (J) The SM appears similar to a tassel branch. (**K** to **N**) SEM of *bd1* mutant tassel. (K) Early stage of SM development. Arrowhead notes axillary branching event. (L) Later stage showing development of an additional meristem (SM) in the axil of a glume. (M) Side view showing distichous phyllotaxy of initiated SM. Numbers correspond to order of initiation. (N) Dissected SM with outer glume removed to show floral organ initiation. OG, outer glume; St, stamen; C, carpel; Si, silk. Scale bar is ~100 μm.

[1]Plant Gene Expression Center, U.S. Department of Agriculture–Agricultural Research Service, 800 Buchanan Street, Albany, CA 94710, USA. [2]Pioneer Hi-Bred International, Johnston, IA, 50131, USA. [3]University of Missouri–St. Louis, 8001 Natural Bridge Road, St. Louis, MO 63121, USA. [4]Division of Biological Sciences, University of California at San Diego, La Jolla, CA 92093-0116, USA.

*To whom correspondence should be addressed. E-mail: gchuck@nature.berkeley.edu

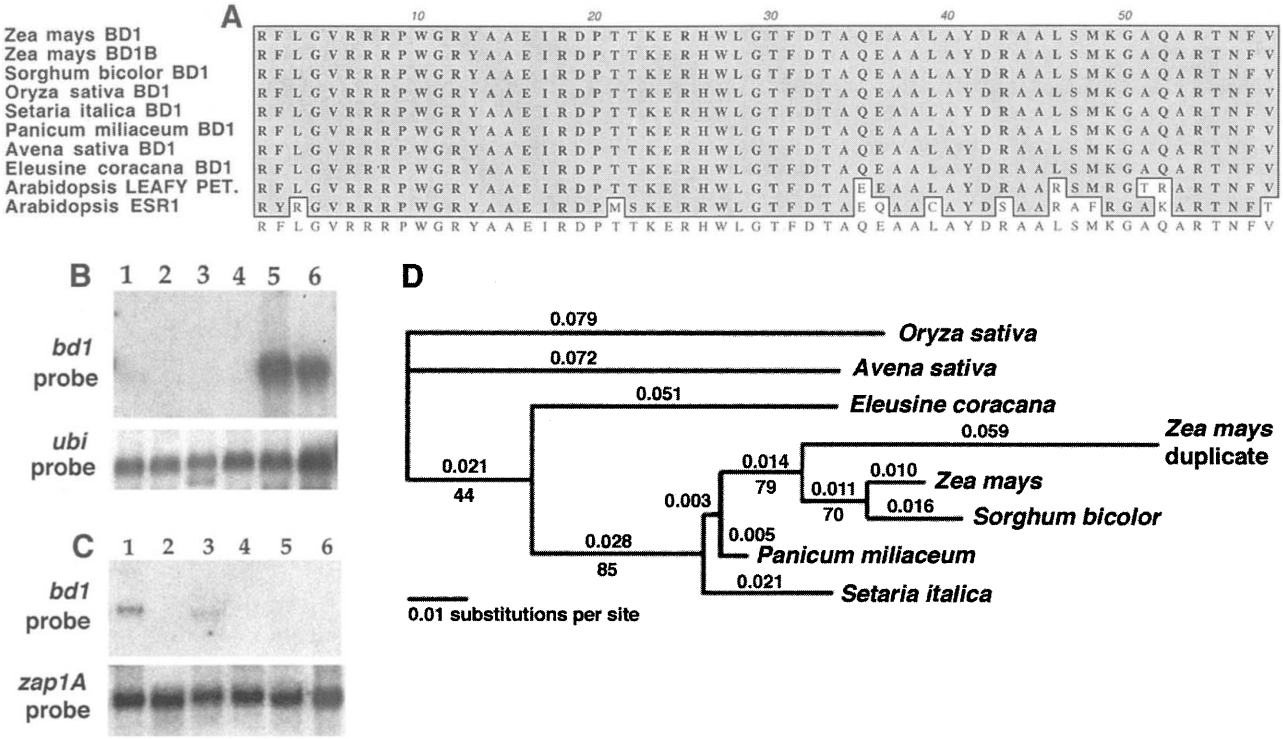

Fig. 2. Sequence and expression of *bd1*. (**A**) ClustalW alignment of the ERF domains of BD1, the duplicate locus BD1B, putative orthologs from other grasses, and the *Arabidopsis* LEAFY PETIOLE and ESR1 proteins. (**B**) Northern blot with 2 μg of poly(A)$^+$ RNA from maize inbred OH43 root (lane 1), leaf (lane 2), embryo (lane 3), shoot (lane 4), tassel (lane 5), and ear (lane 6) tissue probed with the 3′ UTR of the *bd1* cDNA. (Bottom) Hybridization with the maize *ubiquitin* cDNA. (**C**) Northern blot with 1 μg of poly(A)$^+$ RNA from 0.5-cm ears of OH43 (lane 1), *bd1-2* (lane 2), *bd1-mum::20250* (lane 3), *bd1-N2355* (lane 4), *bd1-ref* (lane 5), and *bd1-3* (lane 6). (Bottom) Hybridization with the *zap1a* cDNA (*24*). (**D**) Maximum likelihood tree of the grass *bd1*-like genes excluding regions of ambiguous alignment. Numbers above branches are branch lengths (substitutions per site); numbers below branches are bootstrap values.

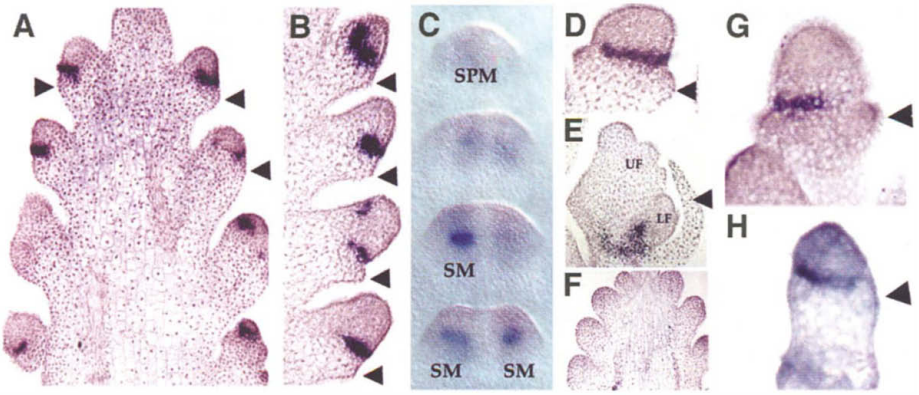

Fig. 3. RNA in situ hybridization of the *bd1* gene. (A to F) maize *bd1* antisense. (**A**) Longitudinal section of a wild-type tassel primordium showing expression at the outer glume/SM junction. Arrowheads denote the outer glume. (**B**) Longitudinal section of a wild-type ear primordium. (**C**) Whole mount in situ of an SPM from a wild-type ear primordium. (**D**) Radial section of a wild-type tassel SM showing an arc of *bd1* expression at the inner glume/SM junction. (**E**) Wild-type ear spikelet showing *bd1* expression at the base of the floral meristems. (**F**) *bd1-2* ear. (**G**) Sorghum SM probed with sorghum *bd1* antisense. (**H**) Rice SM probed with rice *bd1* antisense. uf, upper floret; lf, lower floret.

genes operate in hormone-related pathways.

To determine the tissue-specific expression pattern of *bd1*, the 3′ UTR of the cDNA, which shares no sequence identity with *bd1b*, was used to probe RNA blots (Fig. 2B). A single transcript was detected only in ear and tassel tissue. No *bd1* transcript was detected in the *bd1-N*, *bd1-2*, *bd1-3*, and *bd1-ref* alleles (Fig. 2C). The weak *bd1-mum::20250* allele displayed reduced transcript of a slightly smaller size, consistent with studies of *Mu1* insertions into 5′ untranslated leaders (*13*).

In situ hybridization experiments localized the *bd1* transcript to a semicircular domain at the glume and meristem junction in wild-type ear and tassel inflorescences (Fig. 3, A and B). Expression initiates between the SM and the outer glume and is then detected between the SM and inner glume (Fig. 3D). No expression was observed in the IMs, SPMs, or floral meristems. Whole-mount in situ hybridizations show that *bd1* expression begins soon after the first SM initiates from the SPM and becomes localized to a semicircular domain at the base of the SM above the outer glume (Fig. 3C). Later, this expression domain persists at the base of the developing florets (Fig. 3E). As controls, the sense probe used with wild-type tissue showed no signal (*5*), and the antisense probe on *bd1-2* ears also gave no signal (Fig. 3F). We observed similar expression patterns in the SMs of sorghum and rice using the 3′ ends of their respective *bd1* genes as antisense probes (Fig. 3, G and H).

We propose that BD1 functions to specify SM identity by repressing indeterminate branch fates within the lateral domain of the SM. Like other class two ERF proteins of *Arabidopsis* (*8*), BD1 may accomplish this task by acting as a transcriptional repressor. In one scenario, the zone of *bd1* expression may form a boundary that prevents the ectopic expression of other meristem identity genes in the SMs. In another scenario, BD1 may repress the axillary meristem of the

glume, which can secondarily alter the fate of the SMs when de-repressed.

None of these models adequately address the fact that the *bd1* SM has different fates in the tassel and ear. It is unlikely that *bd1b* partially compensates for the loss of BD1 in the tassel, as proposed for the *zag1/zmm2* duplication in maize (*14*), because we have been unable to detect *bd1b* transcript in any tissues (*15*). It is possible that a different tassel-specific factor may function redundantly with *bd1*. Given the intense selective pressure on the maize ear, it is not surprising that the ear and tassel are genetically distinct.

The expression pattern and mutant phenotype of *bd1* show similarities to the *FIMBRIATA/UFO* genes of *Antirrhinum* and *Arabidopsis*, respectively (*16*, *17*). Both genes are expressed in a ring at the base of the floral meristem adjacent to the sepals, and the *Antirrhinum* mutant shows a partial loss of lateral determinacy within the meristem. In the case of *UFO*, the basal floral meristems may be replaced with coflorescence branches (*18*). In *Arabidopsis*, the *UFO* and *LEAFY* genes have been proposed to be coregulators of floral meristem identity (*19*). Therefore, BD1 may interact with other SM identity factors to impose determinate meristem fates. As in wild type, the maize *LEAFY* ortholog is expressed in the SPMs and SMs of *bd1* mutants (*5*). However, the genetic interaction between *bd1* and *leafy* is unknown and awaits identification of *leafy* mutants in maize.

To date, *bd1* is the only maize mutant that specifically displays altered SM identity. Several maize mutants that affect SM determinacy have been described, such as *Tasselseed6* (*20*) and *indeterminate spikelet1* (*21*). Both these mutants display SMs that initiate more than two florets per spikelet, and interestingly, both show normal patterns of *bd1* expression in the SM (fig. S1). The latter result indicates that SM identity is acquired before SM determinacy. Recently, it has been shown that SM identity and determinacy are interdependent, as two genes that control SM determinacy, *indeterminate spikelet1* and *indeterminate floral apex1*, also show SM identity defects as a double mutant (*22*).

The grass spikelet is conventionally interpreted as a strongly contracted branch system—literally, a little spike (*23*). If this interpretation is correct, then genes should exist that, when mutated, cause the spikelet to revert to a branchlike structure. We have identified a gene that regulates spikelet versus branch meristem fates within the inflorescence of maize, and whose sequence and expression are conserved in other grasses such as rice and sorghum. Our data suggest that the expression of *bd1* is fundamental to grass spikelet formation and may have played a role in the origin of this evolutionary novelty.

References and Notes

1. P. McSteen, D. Laudencia-Chingcuanco, J. Colasanti, *Trends Plant Sci.* **5**, 61 (2000).
2. P. C. Cheng, R. I. Greyson, D. B. Walden, *Am. J. Bot.* **70**, 450 (1983).
3. J. H. Kempton, *J. Hered.* **25**, 29 (1934).
4. L. Colombo *et al.*, *Plant J.* **16**, 353 (1998).
5. Materials and methods are available as supporting material at *Science* Online.
6. T. Helentjaris, D. Weber, S. Wright, *Genetics* **118**, 353 (1988).
7. S. Mathews, R. J. Mason-Gamer, R. E. Spangler, E. A. Kellogg, *Int. J. Plant Sci.* **163**, 441 (2002).
8. S. Y. Fujimoto, M. Ohta, A. Usui, H. Shinshi, M. Ohme-Takagi, *Plant Cell* **12**, 393 (2000).
9. J. L. Riechmann, E. M. Meyerowitz, *Biol. Chem.* **379**, 633 (1998).
10. E. van der Graaff, A. D. Dulk-Ras, P. J. Hooykaas, B. Keller, *Development* **127**, 4971 (2000).
11. K. Wilson, D. Long, J. Swinburne, G. A. Coupland, *Plant Cell* **4**, 659 (1996).
12. H. Banno, Y. Ikeda, Q.-W. Niu, N.-H. Chua, *Plant Cell* **13**, 2609 (2001).
13. A. Barkan, R. Martienssen, *Proc. Natl. Acad. Sci. U.S.A.* **88**, 3502 (1991).
14. M. Mena *et al.*, *Science* **274**, 1537 (1996).
15. G. Chuck, unpublished observations.
16. R. Simon, R. Carpenter, S. Doyle, E. Coen, *Cell* **78**, 99 (1994).
17. G. C. Ingram *et al.*, *Plant Cell* **7**, 1501 (1995).
18. J. Z. Levin, E. M. Meyerowitz, *Plant Cell* **7**, 529 (1995).
19. I. Lee, D. S. Wolfe, O. Nilsson, D. Weigel, *Curr. Biol.* **7**, 95 (1997).
20. E. E. Irish, *Am. J. Bot.* **84**, 1502 (1997).
21. G. Chuck, R. Meeley, S. Hake, *Genes Dev.* **12**, 1145 (1998).
22. D. Laudencia-Chingcuanco, *Development* **129**, 2629 (2002).
23. W. D. Clayton, in *Reproductive Versatility in the Grasses*, G. P. Chapman, Ed. (Cambridge Univ. Press, Cambridge, 1990), pp. 32–51.
24. M. Mena, M. A. Mandel, D. R. Lerner, M. F. Yanofsky, R. J. Schmidt, *Plant J.* **8**, 845 (1995).

25. We thank I. Murray, C. Whipple, and M. Ritter for technical assistance, and members of the Hake laboratory and J. Fletcher for comments on the manuscript. This work was supported by grants from the National Science Foundation to R.S. and S.H.

Supporting Online Material

www.sciencemag.org/cgi/content/full/298/5596/1238/DC1
Materials and Methods
Fig. S1

2 August 2002; accepted 17 September 2002

The IκB–NF-κB Signaling Module: Temporal Control and Selective Gene Activation

Alexander Hoffmann,[1]* Andre Levchenko,[2]* Martin L. Scott,[3]† David Baltimore[1]‡

Nuclear localization of the transcriptional activator NF-κB (nuclear factor κB) is controlled in mammalian cells by three isoforms of NF-κB inhibitor protein: IκBα, -β, and -ε. Based on simplifying reductions of the IκB–NF-κB signaling module in knockout cell lines, we present a computational model that describes the temporal control of NF-κB activation by the coordinated degradation and synthesis of IκB proteins. The model demonstrates that IκBα is responsible for strong negative feedback that allows for a fast turn-off of the NF-κB response, whereas IκBβ and -ε function to reduce the system's oscillatory potential and stabilize NF-κB responses during longer stimulations. Bimodal signal-processing characteristics with respect to stimulus duration are revealed by the model and are shown to generate specificity in gene expression.

The transcription factor NF-κB regulates numerous genes that play important roles in inter- and intracellular signaling, cellular stress responses, cell growth, survival, and apoptosis (*1*–*3*). As such, the specificity and temporal control of gene expression are of crucial physiological interest. Furthermore, the realization of the potential of NF-κB as a drug target for chronic inflammatory diseases or within chemotherapy regimens (*4*, *5*) is dependent on understanding the specificity mechanisms that govern NF-κB–responsive gene expression.

Five related mammalian gene products participate in NF-κB functions (RelA/p65, cRel, RelB, p50, p52), but the predominant species in many cell types is a p65:p50 heterodimer. Its activity is largely controlled by three IκB isoforms (IκBα, -β, and -ε) that bind to NF-κB, preventing its association with DNA and causing its localization to the cytoplasm. Signals from various stimuli are transduced to the IκB kinase (IKK) complex, which phosphorylates each IκB isoform, leading to its ubiquitination and proteolysis (*6*). IκB degradation allows NF-κB to translocate to the nucleus and bind DNA (Fig. 1A). The specific role of each IκB protein in regulating NF-κB is not understood. Mice

[1]Division of Biology, California Institute of Technology, Pasadena, CA 91125, USA. [2]Department of Biomedical Engineering, Johns Hopkins University, Baltimore, MD 21218, USA. [3]Department of Biology, Massachusetts Institute of Technology, Cambridge, MA 02139, USA.

*These authors contributed equally to this work.
†Present address: Biogen, Incorporated, Cambridge, MA 02142, USA.
‡To whom correspondence should be addressed. E-mail: baltimo@caltech.edu